Polymer (Korea) Vol. 16, No. 1, pp 105-114 (1992)

열방성 액정폴리에스테르의 구조 해석

홍 성 권
충남대학교 공과대학 고분자공학과
(1991년 10월 16일 접수)

Structure Analysis of The Thermotropic Liquid Crystalline Copolyester

Sung-Kwon Hong
Dept. of Polymer Science & Engineering, Chungnam National University, Taejon 305-764, Korea
(Received October 16, 1991)

요 약 : 열방성 액정폴리에스터, poly(phenyl-p-phenylene-terephthalate)의 as-spun 상태에서의 구조를 X-선 회절 및 분자모델링 방법을 이용하여 해석하였다. Terephthaloyl chloride(TPA)와 phenylhydroquinone(PHQ)으로부터 합성된 poly(TPA-PHQ)의 as-spun 상태에서의 X-선 회절 구조는 nematic 상태와 3차원 결정상태(crystalline)의 중간쯤의 뒤틀린(distorted) 상태의 구조를 나타내었다. 구조 해석을 위해서는 먼저 single chain의 X-선 회절강도를 cylindrically averaged Fourier transform에 의해 계산하였으며 chain conformation에 의한 효과를 random 상태와 rigid 상태의 chain model에 대해 각각 적용하여 비교하였다. 한편, chain들이 packing 될때 일어나는 interchain interference 효과는 각 chain들의 주축상의 분포를 평균편차를 가진 정규분포함수 개념을 적용하여 고려하였으며 결국, 이들이 구조의 결정화(crystallinity) 정도에 미치는 영향을 chain들의 주축간 분포정도와 관련지어 모형화 할 수 있었으며, 그러한 주축상의 chain들의 규칙적 분포정도(axial register)의 조절을 통한 현구조의 모형화가 가능함을 보여주었다.

Abstract : The structure of the thermotropic copolyester, poly(phenyl-p-phenylene-terephthalate) in the as-spun state, has been studied by X-ray diffraction techniques and molecular modelling. Poly (TPA-PHQ) in the as-spun state, prepared from terephthaloyl chloride(TPA) and phenylhydroquinone(PHQ), has a distorted structure somewhere between the nematic and highly crystalline state. Cylindrically averaged Fourier transform of a single chain has been calculated and the effect of chain conformation on the intensity transform has been studied for the complete random and rigid chain models. The interference effect that occur when chains are packed has also been considered with the release of perfect axial register by introducing a normal distribution function, with standard deviation σ. Thus It has been shown that the diffraction characteristics which we associate with the crystallinity can be generated with the introduction of minimal axial register.

INTRODUCTION

In previous paper,[1] the crystalline structure of poly(phenyl-p-phenylene-terephthalate)[2] was determined by linked-atom least square methods (LALS),[3] based on the X-ray fiber diffraction data for the annealed state. Annealing leads to the development of sharp Bragg reflections, pointing to an ordered three dimensional structure for the copolymer. However, the X-ray fiber diagram of as-spun state, which is shown in Figure 1, shows the scattered intensity largely along the meridian and equator, with only a few diffuse off-equatorial reflections. The scattered intensity along the meridian and equator shows relatively little arching, which indicates a high degree of axial orientation. Meridionals are also observed on the first and third layers, which are absent in the annealed structure due to systematic absence along the fiber. It appears that the molecules in the as-spun state form some sort of quenched nematic structure, except that there are some regions of three dimensional order giving rise to the Bragg reflections.

The equatorial and off-equatorial reflections are at d-spacings similar to those observed for the annealed state, and hence the as-spun fibers probably has an analogous monoclinic (pseudo orthorhombic)[1] lattice of staggered chains packing with interleaved side chains in the unit cell. Since twisted chain packing can be simulated by rotation of the chain, its diffraction can be modelled by cylindrically averaged Fourier transform of a single chain. The approach of Chivers et al.[4,5] for calculating the cylindrically averaged transform has been generallized for multicomponent copolymers and then applied to the present system, which has a periodic alternating backbone. Thereafter, the effect of chain conformation on the intensity transforms has been studied. Then the interference effects that occur when chains are packed with their origins in a $M_1 \times M_2$ array of three dimensional lattice[6] has also been considered.

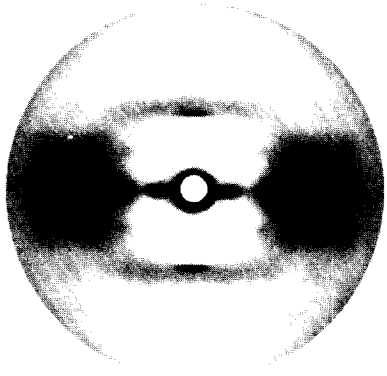

Fig. 1. X-ray diffraction pattern for melt-spun fibers of poly (phenyl-p-phenylene-terephthalate) in as-spun state.

The approach of Blackwell et al.[7~11] for analysis of copolymers has been applied to the present system, in which the interference condition becomes Laue function due to the periodicity in the main chain. The condition of perfect axial register was released by introducing a normal distribution function, with standard deviation σ. The theoretical approach and the results are described in the following.

Cylindrically Averaged Intensity Transforms

The intensity from a three dimensional arrangement of N atoms in space is given by :

$$I(X, Y, Z) = F(X, Y, Z)F^*(X, Y, Z) \quad (1)$$

where :

$$F(X, Y, Z) = \sum_{J=1}^{N} f_j \exp[2\pi i(Xx_j + Yy_j + Zz_j)] \quad (2)$$

and * denotes the complex conjugate. f_j is the atomic scattering factor of the j^{th} atom having coordinates x_j, y_j, z_j, and X, Y, Z are the reciprocal space coordinates. Since we are considering diffraction by fibers, it is more convenient for us to use cylindrical polar coordinates in which z corresponds to the fiber axis, and then equation 2 can be rewritten as :

$$F(R, \Psi, Z) = \sum_{J=1}^{N} f_j \exp[2\pi i\{r_j R\cos(\Psi - \phi_j) + Zz_j\}] \quad (3)$$

where r_j, ϕ_j, z_j and R, Ψ, Z are the real space ato-

mic coordinates and reciprocal space coordinates, respectively. The intensity is given by :

$$I(R, \Psi, Z) = F(R, \Psi, Z)F^*(R, \Psi, Z)$$
$$= \sum_j \sum_k f_j f_k \exp[2\pi i\{r_j R\cos(\Psi-\phi_j) - r_k R\cos(\Psi-\phi_k) + Z(z_j-z_k)\}] \quad (4)$$

For fiber symmetry, there will be cylindrical averaging of I(R, Ψ, Z) and the fiber diagram is a representation of the two dimensional intensity, I(R, Z). Chivers and Blackwell[4,5] have derived equations for the diffracted intensity from copolymer chains at two extremes of the possible conformation :

(a) an extended random conformation for which there is a completely random set of torsion angles between the planar aromatic and ester group in the chain. This corresponds approximately to cylindrically averaging each monomer residue independently in real space, as is shown schematically in Figure 2(a). The resulting chain would have a cylindrical cross section with no rotational correlation between adjacent monomers. The intensity distribution from such a chain is given by :

$$I(R, Z) = \sum_A \sum_B \sum_d Q_{AB}(Z_d)[A_{AB}(R, Z)\cos 2\pi Z z_d + B_{AB}(R, Z)\sin 2\pi Z z_d] \quad (5)$$

where

$$A_{AB} = \sum_j \sum_k f_{A,j} f_{B,k} J_o(2\pi R r_{A,j}) J_o(2\pi R r_{B,k}) \cos 2\pi Z(z_{A,j}-z_{B,k}) \quad (6)$$

and $B_{AB}(R, Z)$ is the equivalent sine term. $Q_{AB}(z_d)$ defines the probability of finding a residue of type A at a distance z_d from a residue of type B. The first summation is for all such z_d separations and the second and third summations cover all residue pairs. The subscripts A, j and B, k denote the j^{th} atom of monomer A and the k^{th} atom of monomer B. Jo is the zeroth order Bessel function for the argument specified. A_{AB} and B_{AB} are the real and imaginary components of the Fourier transform of the cross convolution of residue B with residue A when both residues are cylindrically averaged.

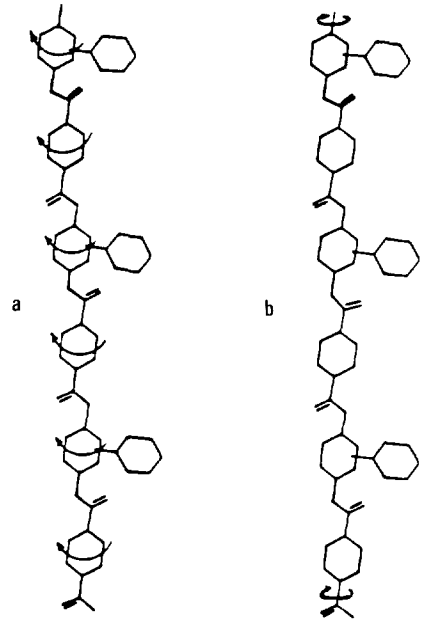

Fig. 2. (a) Schematic representation of cylindrical averaging of monomers for an extended random conformation model of the copolymer chain. (b) Schematic representation of cylindrical averaging of the entire chain leading to the extended rigid conformation model.

(b) an extended rigid conformation with specific torsion angles repeated along the chain. In this example as is shown in Figure 2(b), the aromatic-ester and ester-aromatic torsion angles were set at -7.3° and 65.5°,[1] respectively. The presence of off-equatorial Bragg reflections in x-ray fiber diagram points to the presence of some regular three dimensional packing, which will require an ordered conformation for at least part of the structure. In this case of rigid conformation, I(R, Z) is derived by cylindrically averaging of the full three dimensional intensity transform I(R, Ψ, Z) in reciprocal space. I(R, Z) has the same form as equation 5 except that $A'_{AB}(R, Z)$ and $B'_{AB}(R, Z)$ are defined as sums over n^{th} order Bessel functions of the first kind.

$$I(R, Z)=\sum_A \sum_B \sum_d Q_{AB}(Z_d)[A'_{AB}(R, Z)\cos 2\pi Z z_d + B'_{AB}(R, Z)\sin 2\pi Z z_d] \quad (7)$$

where

$$A'_{AB}=\sum_j \sum_k f_{A,j}f_{B,k}J_n(2\pi R r_{A,j})J_n(2\pi R r_{B,k}) \cos[n(\phi_{A,j}-\phi_{B,k})+2\pi Z(z_{A,j}-z_{B,k})] \quad (8)$$

and $B'_{AB}(R, Z)$ is the equivalent sine term.

the above calculation can be simplified by modelling the chain as a paracrystalline lattice with random coordination statistics for the constituent polyatomic monomers, and equation 6 can be written as :

$$I(R, Z)=\sum_A P_A F_{AA}(R, Z) + 2\mathrm{Re}\sum_A \sum_B F_{AB}(R, Z)T_{AB}(Z) \quad (9)$$

where

$T_{AB}(Z)$ defines the paracrystalline lattice and represents an element of the matrix T which is defined as follows :

$$T=P.M.X(z)/[I\text{-}M.X(z)] \quad (10)$$

I is a unit matrix and the matrices P, M and X define monomer composition, combination probability and the phase effects associated with the different monomer lengths, respectively. For the extended random conformation, $F_{AB}(R, Z)$ is given by :

$$F_{AB}(R, Z)=\sum_j \sum_k f_{A,j}f_{B,k}J_o(2\pi R r_{A,j})J_o(2\pi R r_{B,k}) \exp 2\pi i Z(z_{B,k}-z_{A,j}) \quad (11)$$

and for the extended rigid conformation, the corresponding $F_{AB}(R, Z)$ is given by :

$$F_{AB}(R, Z)=\sum_{n=-\infty}^{\infty} \sum_j \sum_k f_{A,j}f_{B,k}J_n(2\pi R r_{A,j})J_n(2\pi R r_{B,k}) \exp 2\pi i[(n/2\pi)(\phi_{B,k}-\phi_{A,j})+Z(z_{B,k}-z_{A,j})] = \sum_j \sum_k f_{A,j}f_{B,k}J_o(2\pi R r_{A,j\,B,k}) \exp 2\pi i Z(z_{B,k}-z_{A,j}) \quad (12)$$

For the present poly(phenyl-p-phenylene-terephthalate) system, the matrices P, M and X are defined as follows :

$$P=\begin{bmatrix} P_T & O \\ O & P_H \end{bmatrix} \quad M=\begin{bmatrix} M_{TT} & M_{TH} \\ M_{HT} & M_{HH} \end{bmatrix} \quad X=\begin{bmatrix} X_T & O \\ O & X_H \end{bmatrix}$$

where the subscripts T and H are abbreviations of terephthaloyl chloride and phenyl-hydroquinone, respectively, and for example P_T is the molar composition of monomer T, M_{TT} is the combination probability for dimer TT, and X_T is the phase term for monomer T (and is equal to $\exp 2\pi i Z z_T$).

Interchain Interference Effects

In the case of finite chains, each of N monomers, the scattering in the chain axis (Z) direction by a nematic array of chains of point monomers is given by

$$I_a(Z)=N\mathrm{Re}[(1+H(Z))/(1-H(Z))-2H(Z) (1-H^N(Z))/N(1-H(Z))^2] \quad (13)$$

where Re designates the real component and H (Z) is the Fourier transform of the first neighbor probability distribution along the Z (chain axis) direction. In the case of infinite chains, equation 13 becomes

$$I_a(Z)=\mathrm{Re}[(1+H(Z))/(1-H(Z))] \quad (14)$$

To address the interference effects between the neighbor chains, we now consider the two dimensional array of points shown in Figure 3, representing M chains, each of N monomers. In general, the chains are composed of random sequences of two monomers A and B of lengths Z_A and Z_B, and the overall compositions of the monomers are P_A and P_B. The separation between chains in the X direction is a. The total scattering intensity can be separated into intra (1) and intermolecular (2) components

$$I(X, Z)=I_1(X, Z)+I_2(X, Z) \quad (15)$$

The intramolecular component $I_1(X, Z)$ is simply M times $I_a(Z)$ in equation 13, and the intermolecular component $I_2(X, Z)$, which accounts for the interference effects between chains, can be written as a summation over the interferences between

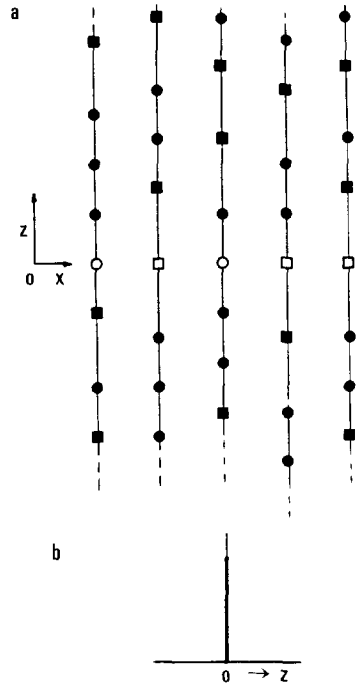

Fig. 3. (a) A two dimensional arrangement of chains with the origin monomers (unshaded) lying on the x-axis. (b) Distribution of origin monomers about the x-axis.

the 1st, 2nd, 3rd, etc. nearest neighbor chains.

$$I_2(X, Z)=\sum_{m-1}^{M-1}(M-m)I_2^m(X, Z) \quad (16)$$

where the $I_2^m(X, Z)$ terms represent the interferences between the m^{th} nearest neighbor chains, i.e. the i^{th} and $i+m^{th}$ chain which are separated by a distance ma, and there will be M-m such interferences.

$$I_b(Z)=\frac{1-K^N(Z)}{1-K(Z)} + 2Re\left[\frac{H(Z)}{K(Z)-H(Z)}\left[\frac{1-K^N(Z)}{1-K(Z)}-\frac{1-H^N(Z)}{1-H(Z)}\right]\right] \quad (17)$$

Now the total scattering intensity in equation 15 can be expressed as

$$I(X, Z)=MI_a(Z)+I_b(Z)I_c(X) \quad (18)$$

where

$$I_c(X)=2\sum_{m-1}^{M-1}(M-m)\cos(2\pi Xma) \quad (19)$$

and when the chains are periodic, the above equation becomes a Laue function. For a three dimensional $M_1 \times M_2$ array of chains separated by a along the x-axis and b along the y-axis in an orthorhombic lattice,[5] equation 18 ia expressed as

$$I(X, Y, Z)=M_1M_2I_a(Z)+I_b(Z)I_c(X, Y) \quad (20)$$

where

$$I_c(X, Y)=4\sum_{m_1=0}^{N-1}{}'\sum_{m_2=0}^{N-1}{}'(M_1-m_1)(M_2-m_2)\cos(2\pi Xm_1a)\cos(2\pi Ym_2b) \quad (21)$$

and the primes under the summation signs indicate that the term $m_1=m_2=0$ is omitted from the summation and that the terms $m_1=0$, $m_2=0$ and $m_1=0$, $m_2=0$ are given half-weight only.

In the above section the condition of perfect register was assumed by setting an origin monomer in each chain in a plain, but that condition can be released by introducing a distribution function to describe the probability that an origin monomer will be in the reference plane as shown in Figure 4. To incorporate this probability a normal distribution, G(Z), with standard deviation σ has been used

$$G(Z)=1/\sqrt{2\pi}\,\sigma\exp[-z^2/2\sigma^2] \quad (22)$$

The Fourier transform of G(Z) is represented as A(Z) where

$$A(Z)=F[G(Z)]=\exp[-2\pi^2Z^2\sigma^2] \quad (23)$$

Such deviation from register only affect the intermolecular interference, and is incorporated into equation 18 via the convolution theorem :

$$I(R, Z)=MI_a(Z)+A(Z)I_b(Z)I_c(R) \quad (24)$$

EXPERIMENTAL

Synthesis

The polymer was synthesized from equimolar quantities of terephthaloyl chloride and phenylhy-

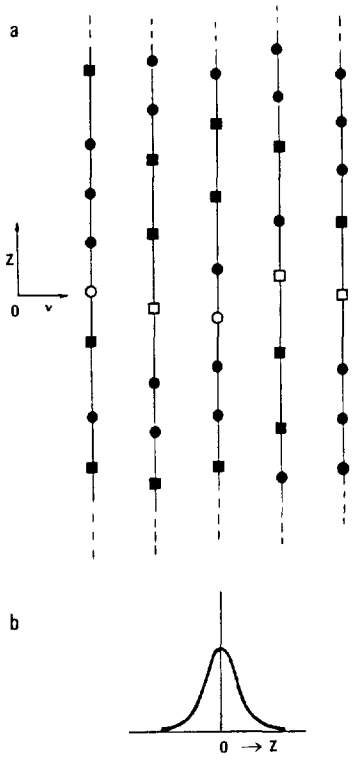

Fig. 4. (a) A two dimensional arrangement of copolymer chains with the origin monomers distributed about the x-axis. (b) A Gaussian distribution defining the position of origin monomers about the x-axis.

droquinone dissolved in methylene chloride in the presence of pyridine as an acid trap. Phenylhydroquinone and terephthaloyl chloride (reagent grades) were obtained from Eastman Kodak and Sigma Chemical Co., respectively. The reaction was conducted under a moderate nitrogen-flow blanket at approximately atmospheric pressure. The terephthaloyl chloride was added slowly to the phenylhydroquinone solution while stirring vigorously and maintaining the temperature at approximately 0℃. Upon completion of the polymerization, the solvent was extracted by distillation. The solid product was washed with water and acetone several times, filtered and dried in a vacuum oven at approximately 100℃ and 500 mmHg overnight. The dried polymer had a melting point of about 350℃ and inherent viscosity of 0.45 dl/g when dissolved in equal volumes of trifluoroacetic acid and methylene chloride.

X-ray Diffraction

Specimens for X-ray analysis were bundles of parallel fibers drawn by hand from the melt. These were examined both in the as-spun state and after they had been annealed at 250℃ for 2 hours. X-ray fiber diagrams were recorded on Kodak no-screen X-ray film using Ni-filtered CuK α radiation and a Searle toroidal focusing camera. Calibrations were made by using calcium fluoride. The X-ray fiber diffraction pattern of as-spun sample is shown in

Table 1. Cylindrical Polar Atomic Coordinates of Monomers

Atom	r(Å)	φ(rad)	z(Å)
TPA			
01	0.00	0.00	0.00
02	2.21	-1.57	0.71
C0	1.03	-1.57	0.91
C1	0.51	-1.57	2.30
C2	0.87	1.39	2.48
C3	1.39	1.46	3.76
C4	0.55	1.56	4.86
C5	0.83	-1.75	4.68
C6	1.35	-1.68	3.40
C7	1.05	1.57	6.26
04	2.19	1.57	6.60
03	0.00	0.00	7.14
PHQ			
03	0.00	0.00	0.00
C8	0.00	-1.53	1.41
C9	1.19	1.57	2.13
C10	1.16	1.57	3.51
C11	0.05	-1.57	4.18
C12	1.24	-1.57	3.47
C13	1.22	-1.57	2.08
C14	2.50	1.57	1.41
C15	3.00	1.22	0.54
C16	4.16	1.32	-0.13
C17	4.92	1.57	0.06
C18	4.72	1.79	0.92
C19	3.55	1.87	1.59
05	0.00	0.00	5.59

Figure 1.

Molecular Modelling and Intensity Transforms

Table 1 lists the cylindrical polar coordinates of the TPA and PHQ residues, arranged with their terminal ester oxygens on the z-axis. Figure 5 shows these conformations, the numbering of the atoms and the torsion angles. I(R, Z) was calculated for infinite chains of the two monomers in the random and rigid conformations. All torsion angles are defined as positive for anti-clockwise rotation, and 0℃ corresponds to the cis-conformation in each case. $\Psi_1(=\Psi_2)$ is set at -7.3℃ and $\Psi_3(\Psi_4)$ is set at 65.5°. The phenyls are at the 2- and 3-positions and weighted by 0.5. For the phenyl side chains, the torsion angles are first set at 60°. Later random rotational averaging of the phenyls was considered by positioning 18 phenyls on each carbon (2- and 3-) separated by 10° intervals of Φ and weighted by about 0.028 (=0.5/18). The matrices which define the interference function for the alternating copolymer are given as follows :

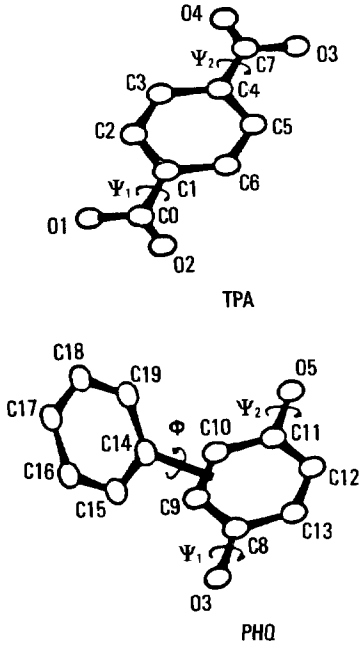

Fig. 5. Projection of the model structures of the monomers, TPA and PHQ. Ψ_1 and Ψ_2 are the ester-aromatic and aromatic-ester torsion angles, respectively.

$$P=\begin{bmatrix}0.5 & 0\\ 0 & 0.5\end{bmatrix} \quad M=\begin{bmatrix}0 & 1\\ 1 & 0\end{bmatrix}$$

$$M=\begin{bmatrix}\exp 2\pi i Z z_T & 0\\ 0 & \exp 2\pi i Z z_H\end{bmatrix}$$

To consider the interchain interference effects, 200 average chains, each of 30 repeat units, were considered for the calculation. The chains were considered as an pseudo-orthorhombic array of two chains with a=12.81 and b=5.1 Å, based on the observed equatorial and off-equatorial reflections. The perfection of axial register was modified by varying σ in equation 22 in 0.5 Å increment from 0 to 2 Å. Random axial stagger as in a nematic array was simulated by using a large value for the standard deviation, i.e. σ=10 Å. The theoretical calculations were done on a 341×341 grid along the positive R and Z axes respectively, but limited to scattering angles of $2\theta<34°$, which covers up to the fourth layer lines on meridian. A value of 255 (the darkest shade) was assigned to all I(R, Z) values higher than 1500 (normalized to the scattering by one average monomer). This simply truncates the high intensity on the equator, so that the weaker intensities can be observed. Values of I(R, Z) less than 1500 were scaled proportionally. The calculated intensities were displayed on the monitor of an AED 512 color terminal and compared with the observed diffraction patterns.

RESULTS AND DISCUSSION

The X-ray fiber diffraction pattern of as-spun sample is shown in Figure 1. Annealing leads to the development of sharp Bragg reflections, pointing to an ordered three-dimensional structure for the copolymer.[1] The presence of off-equatorial Bragg reflections in X-ray fiber diagram points to the presence of some regular three dimensional packing, which will require an ordered conformation for at least part of the structure. The present paper analyses the structure of the as-spun state.

Molecular modelling for an extended random conformation is shown schematically in Figure 2(a), for which there is a completely random set of torsion angles between the planar aromatic and ester group in the chain. Extended rigid conformation with specific torsion angles repeated along the chain is shown in Figure 2(b), for which aromatic-ester and ester-aromatic torsion angles were set at -7.3℃ and 65.5°,[1] respectively.

The two dimensional array of points to adress the interference effects between the neighbor chains is shown in Figure 3, representing M chains, each of N monomers, and the condition which introduces a distribution function to describe the release of perfect register is shown in Figure 4. To incorporate this probability a normal distribution, G(Z), with standard deviation σ in equation 22 has been used. Figure 5 shows the detailed conformations of the TPA and PHQ residues with the numbering of the atoms and the torsion angles.

Figure 6 shows the calculated intensity for a infinite chain of poly(phenyl-p-phenylene-terephthalate) for (a) an extended random conformation and (b) an extended rigid conformation, both as defined above. A line of constant intensity (I=15 00) was assigned to the equator (Z=0). Equation 9 predicts infinite intensity in this region. The calculated intensity for the two extremes of the possible conformations consists primarily of a series of periodic layer lines with a repeat distance of 12. 62 Å, which is consistent with the observed layer line spacing, 12.6 Å. The predicted intensity on the meridian is the same for the two models since at R=0 equation 11 and 12 become identical to each other. The sharpness of the layer lines in the z direction is due to the assumption of an infinite chain and it can be broadened by use of a finite chain length.

The major differences between the random and rigid models lie in the relative intensities and extents of the non-meridional layer lines. In this regard the rigid conformation shows better agreement with the observed pattern as shown in figure

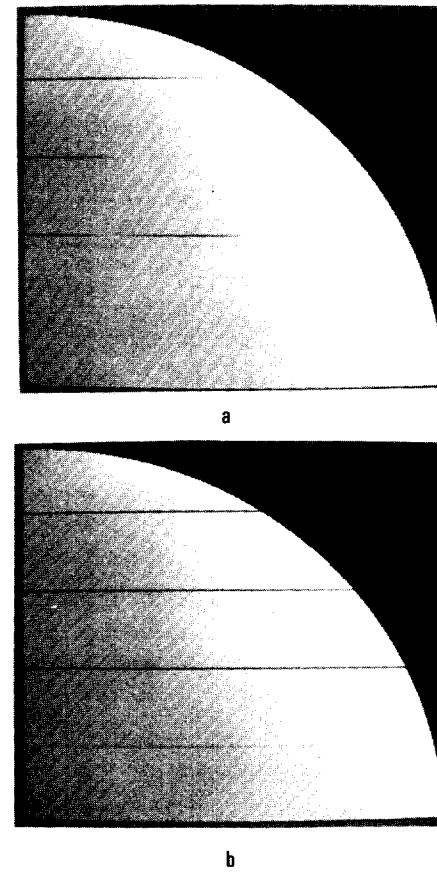

Fig. 6. Calculated fiber patterns for infinite chain of TPA/PHQ for (a) an extended random conformation and (b) an extended rigid conformation of the monomers.

1. Figure 7 shows the calculated diffraction pattern for a nematic array of chains packed on an orthorhombic network with a=12.81 and b=5.1 Å. Random axial stagger is simulated by setting σ=10.0 Å in equation 22 although results are largely indistinguishable for σ > 2.0 Å. The effect of introducing a register plane containing origin atoms on each chain is shown in Figure 8, which correspond to σ=0.0 Å. Most of the observed Bragg maxima have been generated with only minor distortions except, notably, the 100 reflection. This is absent due to the fact that we have two identical chains along the a axis, whereas in reality they are proba-

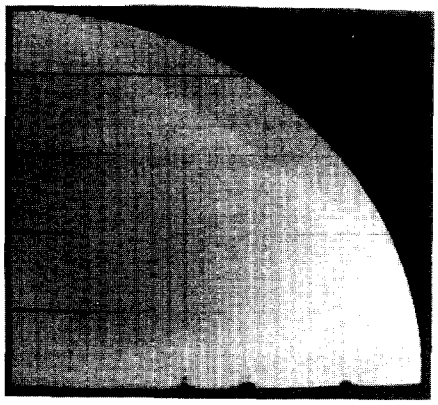

Fig. 7. Calculated diffraction pattern for 200 packed chains with completely random axial stagger simulated by $\sigma = 10.0$ Å.

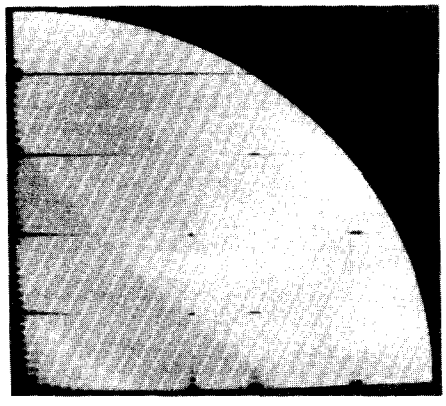

Fig. 8. Calculated diffraction pattern for 200 packed chains with perfect axial stagger ($\sigma = 0.0$ Å).

bly staggered and rotated with respect to the c axis.

Table 2 shows the R, Z comparison between observed and calculated reflections. With registration as defined, we have more extensive ordering than is indicated by the observed data. We need to reduce the order imposed on the model, which can be done by relaxing the requirement that the origin atom must lie on the register plane so as to consider the situation where this registration is probably the case, as defined by the G(Z) normal distribution. Figure 9-10 show the predicted diff-

Table 2. R, Z Comparison Between Observed and Calculated Reflections

	R, Z value of observed ($Å^{-1}$)	R, Z value of calculated ($Å^{-1}$)
Equator	(0.078, 0.000)	-----
	(0.157, 0.000)	(0.155, 0.000)
	(0.220, 0.000)	(0.211, 0.000)
	(0.309, 0.000)	(0.305, 0.000)
1st layer	(0.000, 0.080)	(0.000, 0.079)
	(0.146, 0.080)	(0.155, 0.079)
	(0.212, 0.080)	(0.211, 0.079)
	(0.290, 0.080)	(0.305, 0.079)
2nd layer	(0.000, 0.159)	(0.000, 0.159)
	(0.189, 0.159)	(0.155, 0.159)
	(0.233, 0.159)	(0.211, 0.159)
	-----	(0.305, 0.159)
3rd layer	(0.000, 0.242)	(0.000, 0.241)
	(0.215, 0.242)	(0.210, 0.241)
	-----	(0.305, 0.241)
4th layer	(0.000, 0.325)	(0.000, 0.323)
	-----	(0.155, 0.323)

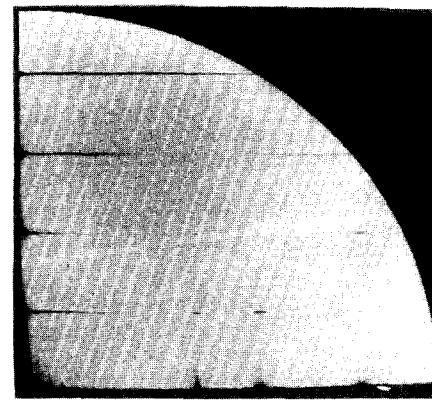

Fig. 9. Calculated diffraction pattern for 200 packed chains with $\sigma = 1.0$ Å.

raction patterns for structures in which the registration is relaxed by setting σ at 1.0 and 2.0 Å, corresponding to progressively wider distributions of the chain origins about the register plane. It can be seen that sharp Bragg reflections cease to occur as σ increases. The results in Figure 9 for $\sigma = 1.0$

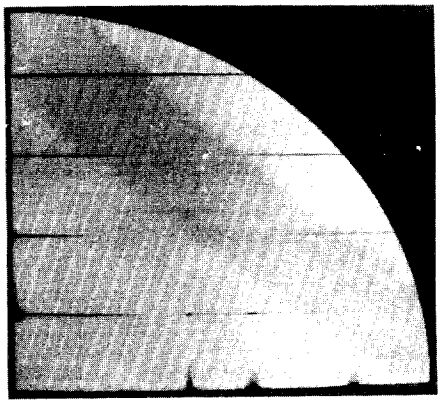

Fig. 10. Calculated diffraction pattern for 200 packed chains with $\sigma=2.0$ Å.

Å compare favorably with the observed patterns for the as-spun fibers. Thus it has been demonstrated that the diffraction characteristics that we associate with crystallinity can be generated with the introduction of minimal register.

Acknowledgements : The author wishes to express sincere gratitude to Dr. John Blackwell in Case Western Reserve University for his invaluable advice and assistance throughout the course of this work.

REFERENCES

1. S. K. Hong and J. Blackwell, *Polymer,* **30,** 225 (1989).
2. C. R. Payet, US Patent 4,159,365 (1979).
3. C. Smith and S. Arnott, *Acta Crystallogr.(A),* **34,** 3 (1978).
4. R. A. Chivers and J. Blackwell, *Polymer,* **26,** 997 (1985).
5. R. A. Chivers, G. A. Gutierrez, and J. Blackwell, *ibid,* **26,** 348 (1985).
6. A. Keller and A. Maradudin, *J. Phys. Chem. Solids.,* **2,** 301 (1957).
7. J. Blackwell, H. M. Cheng, and A. Biswas, *Macromolecules,* **21,** 39 (1988).
8. J. Blackwell, A. Biswas, and R. C. Bonart, *ibid,* **18,** 2126 (1985).
9. J. Blackwell, G. Leiser, and G. A. Gutierrez, *ibid,* **16,** 1418 (1983).
10. J. Blackwell and G. A. Gutierrez, *Polymer,* **23,** 671 (1982).
11. J. Blackwell, G. A. Gutierrez, R. A. Chivers, and W. J. Ruland, *J. Polym. Sci., Polym. Phys. Ed.,* **22,** 1343 (1984).